



Effect of the grain radius on the electrical parameters of an n⁺/p polycrystalline silicon solar cell under monochromatic illumination considering the cylindrical orientation

Assane Diouf^{1,2}, Amadou Diao¹, Senghane Mbodji^{1,2*}

¹Research team in Renewable Energies, Materials and Laser of Department of Physics, Alioune DIOP University of Bambey, Bambey, Senegal

²Laboratory of Semiconductors and Solar Energy, Department of Physics, Faculty of Science and Technology, Cheikh Anta Diop University, Dakar, Senegal

Abstract The cylindrical model is used for the characterization of an n⁺/p polycrystalline silicon solar cell under monochromatic illumination. From this model, the continuity equation of the density of the excess charge carriers has been solved in steady state using the Bessel functions and the dynamic junction velocity (S_f). An expression of the density of the excess charge carriers in the base is obtained as a function of the grain radius (R) and the base depth. This allowed us to establish the photocurrent and the photovoltage expressions that lead to I-V and P-V characteristic curves in which the shunt resistance, R_{sh} , is determined. The effect of the grain radius on the electrical parameters of the solar cell matches fairly well with values reported in the literature.

Keywords cylindrical model, grain radius, shunt resistance

1. Introduction

The non-uniform doping of an n⁺/p type semiconductor, gives rise to the space charge region (SCR). Shockley [1] is the first to model and characterize the space charge region. Extensive studies on this space charge region allowed the development of the concept of the junction recombination velocity (S_f) [2,3] which defines the current flow through the junction corresponding both to the operating point of the solar cell [2,3] and to the intrinsic junction recombination velocity which is related to the shunt resistance [2,3].

From a cylindrical approach, S. Elnahwy and N. Adeeb [4] determined the total photocurrent density of a polycrystalline silicon solar cell and investigated the effect of the grain boundary recombination velocity (S_{gb}) on the spectral response. They showed that for grain boundary recombination (S_{gb}) values greater than 10^4 cm/s, the spectral response decreases significantly. A. Trabelsi et al. [5] determined the analytical expression of the short-circuit current density and that of the dark current. Other authors [2,3,5], using the columnar cubic approach, have proposed some methods of characterization of solar cell. Mbodji et al. [6] presented a new technique based on the junction recombination velocity (S_f) to determine both the shunt (R_{sh}) and series (R_s) resistances of an n⁺/p polycrystalline silicon solar cell. I-V and P-V characteristics were obtained for different values of the junction recombination velocities S_f (0 to 1.510^6 cm/s). Adachi et al. [7] used the dielectric model to determine the electrical properties of an n-CdS / p-CdTe heterojunction solar cell. An optimization of the I-V and P-V characteristics has been studied for different temperature where the shunt (R_{sh}) and series (R_s) resistances were determined. Depending on environmental conditions, these intrinsic parameters (R_{sh} and R_s) act significantly on the maximum power point.

The aim of our study is to enlarge the few works done in cylindrical orientation of the grain of the polycrystalline silicon solar cell. Here, we resolve the continuity equation and study the effect of the grain radius on the electrical parameters.



2. Theory

We represent in figure 1, an n⁺/p type of a cylindrical scheme of the considered polycrystalline silicon solar cell.

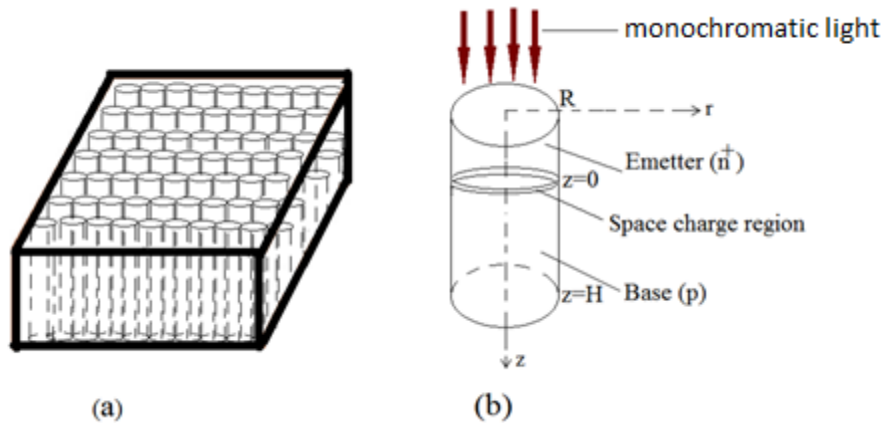


Figure 1: (a) fibrously oriented grain, (b) elementary cylindrical grain solar cell

In figure 1, R is the grain radius and H means the base thickness.

When the solar cell is illuminated along the z axis, photo generation and recombination of the minority carriers occur in the base. Considering the cylindrical coordinates, the behavior of the excess minority carriers' density in the base is governed by the continuity equation [4-5]:

$$\frac{\partial^2 \delta(r, \theta, z)}{\partial r^2} + \frac{\partial^2 \delta(r, \theta, z)}{\partial z^2} + \frac{1}{r^2} \cdot \frac{\partial^2 \delta(r, \theta, z)}{\partial \theta^2} + \frac{1}{r} \cdot \frac{\partial \delta(r, \theta, z)}{\partial r} - \frac{\delta(r, \theta, z)}{L^2} = -\frac{G(z)}{D} \tag{1}$$

With D and L corresponding to the coefficient diffusion and the diffusion length, respectively;

$\delta(r, z)$ is the excess minority carriers' density in the base.

G(z) is the generation rate and is expressed as [6]:

$$G(z) = \alpha \cdot I_0 \cdot (1 - R') \cdot \exp(-\alpha \cdot z) \tag{2}$$

R', I₀ and α are the reflection coefficient, the incident photon flux and the absorption coefficient, respectively.

Taking into account of the symmetry of the angle θ [1, 2], equation (1) becomes:

$$\frac{\partial^2 \delta(r, z)}{\partial r^2} + \frac{\partial^2 \delta(r, z)}{\partial z^2} + \frac{1}{r} \cdot \frac{\partial \delta(r, z)}{\partial r} - \frac{\delta(r, z)}{L^2} = -\frac{G(z)}{D} \tag{3}$$

The solution of the equation (3) is given by equation (4) as:

$$\delta(r, z) = \sum_{k \geq 1}^{\infty} \left[A_k \cdot r + \frac{2 \cdot \alpha \cdot (1 - R)}{H \cdot D(T)} \cdot \frac{L_k^2 \cdot c_k}{c_k^2 + \alpha^2} \cdot G(H) - \frac{2K_k}{L^2(T) \cdot H} \cdot \frac{1 - \cos(c_k \cdot H)}{c_k} \right] \cdot \sin(c_k \cdot z) + K \tag{4}$$

The coefficients A_k, K_k and C_k are determined from the following boundary conditions:

- at the junction (z = 0) [6]:

$$\left. \frac{\partial \delta(r, z)}{\partial z} \right|_{z=0} = \frac{Sf}{D} \cdot \delta(r, z=0) \tag{5}$$

- at the back surface (z = H) [4-6]:

$$\left. \frac{\partial \delta(r, z)}{\partial z} \right|_{z=H} = -\frac{Sb}{D} \cdot \delta(r, H) \tag{6}$$

- at the grain boundary (r = R) [4,5]:



$$\left. \frac{\partial \delta(r, z)}{\partial r} \right|_{r=R} = -\frac{S_{gb}}{D} \cdot \delta(R, z) \tag{7}$$

Where Sf is the junction recombination velocity and is called the dynamic junction velocity [8]; Sb is the back surface velocity and Sgb the grain boundary velocity. The association of Sgb with both Sf and Sb permitted us to have a new expression of the excess minority carriers' density in the base of the solar cell. Hence the study of the solar cell for any real operating condition varying from the open circuit to the short-circuit [6] can be easily done.

2.1. Photocurrent density

The photocurrent density I_{ph} of the excess minority carriers at the junction of the solar cell is given by [6]:

$$I_{ph}(H, R, S_{gb}, Sf, Sb, \lambda) = q \cdot D \cdot \left. \frac{\partial \delta(r, z)}{\partial z} \right|_{z=0} \tag{8}$$

Where q is the elementary charge

2.2. Photovoltage

For a given illumination and according to the Boltzmann's law, the photovoltage V_{ph} is expressed as [9]:

$$V_{ph}(H, R, S_{gb}, Sf, Sb, \lambda) = V_T \cdot \text{Log} \left[N_b \cdot \frac{\delta(H, R, S_{gb}, Sf, Sb, \lambda)}{n_i^2} + 1 \right] \tag{9}$$

N_b = 10¹⁶ cm⁻³ is the doping rate of the base in acceptor atoms; n_i = 10¹⁰ cm⁻³ is the intrinsic minority carriers' density and V_T denotes the thermal voltage and is defined as:

$$V_T = K \cdot \frac{T}{q} \tag{10}$$

Where K is the Boltzmann constant, T is the absolute temperature at thermal equilibrium (T = 300°K).

3. Results and Discussions

The profile of the photocurrent according to the dynamic junction velocity for different grain radius is represented in figures 2.

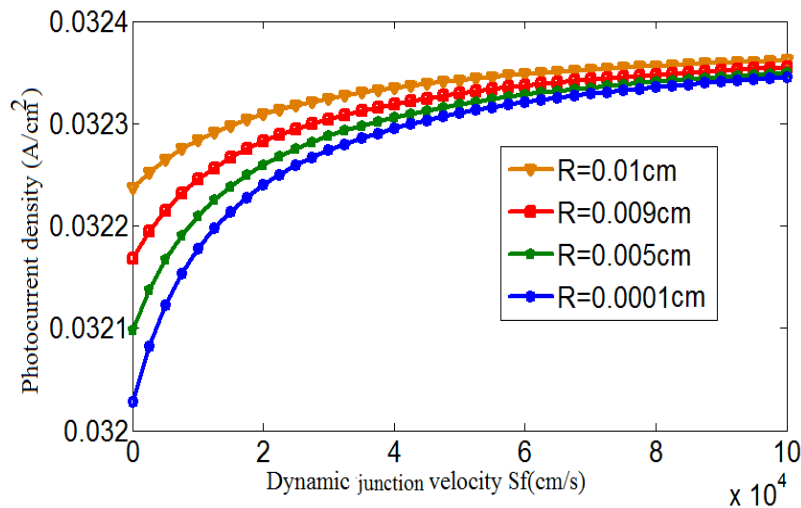


Figure 2: Photocurrent density versus dynamic junction velocity for different grain radius
 D=26cm², Sb=10⁴ cm.s⁻¹, λ=1000 nm, L = 0.01cm, H=0.001cm, Sgb=5000cm.s⁻¹

In figure 2, we noted that the photocurrent density increases with the dynamic junction velocity. The result is similar to those obtained in [3]. But for our model, we remarked that the open circuit operating point is very short while the short-circuit zone is very long meaning that the initiating short-circuit operating condition [10]

could be low. This could hence affect the determination of series and shunt resistances. The model is appropriated for the determination of the shunt resistance but must be adjusted for a good determination of the series resistance.

When increasing the grain radius (R), the magnitude of the photocurrent increases. Findings are in good agreement with [3, 11] and showed that the lower grain radius correspond to an increases of activities in recombination centers leading to decrease the photocurrent and hence the efficiency of the solar cell.

In figures 3, the profile of the photovoltage according to the dynamic junction velocity for different grain radius (R), is represented.

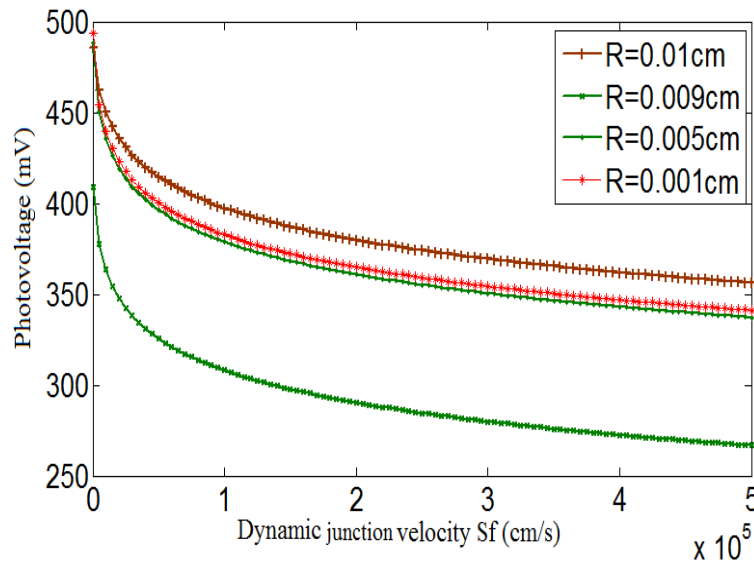


Figure 3: photovoltage versus dynamic junction velocity for different grain radius (R):
 $D=26\text{cm}^2$, $S_b=10^4 \text{ cm.s}^{-1}$, $\lambda=1000 \text{ nm}$, $L = 0.01\text{cm}$, $H=130 \mu\text{m}$, $S_{gb}=5000\text{cm.s}^{-1}$.

The photovoltage, in figure 3, decreases when the dynamic junction velocity increases. The greater values of the photovoltage are obtained around the open circuit situation and the lesser ones in short circuit situation of the solar cell. In open circuit, there is a storage of excess minority carriers density that have not enough energy to cross the junction while in short circuit the excess minority carriers have more energy to cross the junction where they aren't stocked. We noted a decrease of the magnitude of the photovoltage when the grain radius decreases. This result confirms conclusions of [3].

In figures 4 and 5, the I-V and P-V characteristic curves are represented, respectively, for different grain radius when the grain boundary recombination velocity has a fixed value.

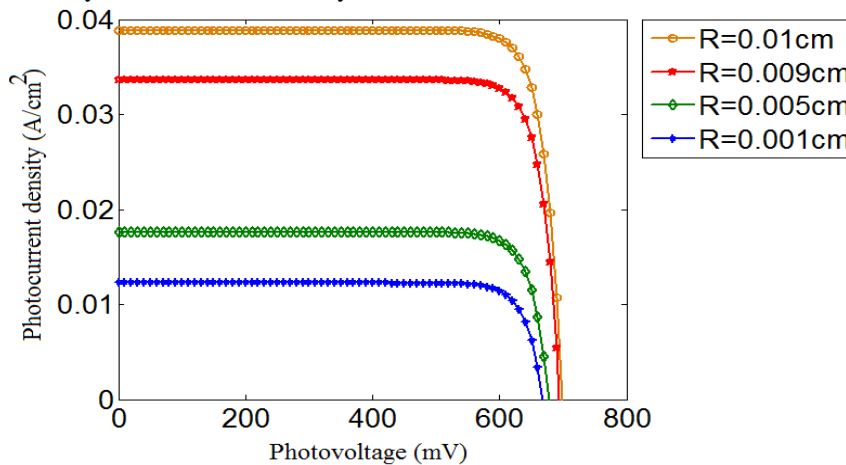


Figure 4: photocurrent density versus photovoltage for different grain radius: $D=26\text{cm}^2.\text{s}^{-1}$; $S_b=10^4 \text{ cm.s}^{-1}$; $\lambda=1000 \text{ nm}$; $L = 0.01\text{cm}$; $H=130 \mu\text{m}$; $S_{gb}=5000\text{cm.s}^{-1}$

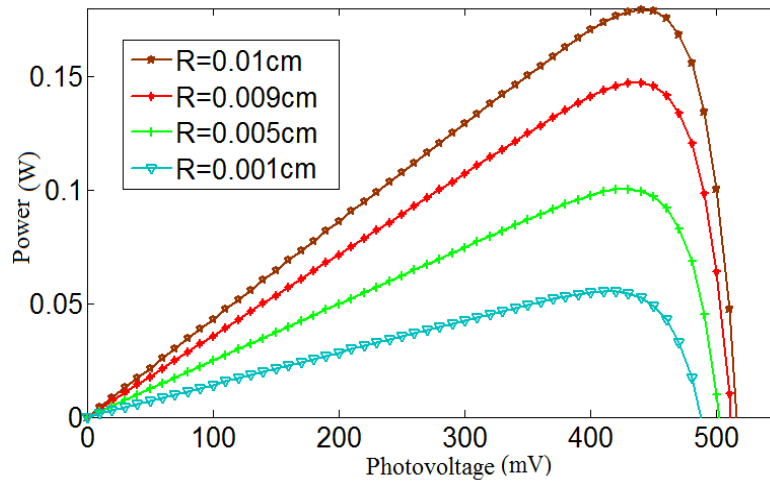


Figure 5: power versus photovoltage for different grain radius: $D=26\text{cm}^2.\text{s}^{-1}$; $S_b=10^4\text{ cm}.\text{s}^{-1}$; $\lambda=1000\text{ nm}$; $L = 0.01\text{cm}$; $H=130\text{ }\mu\text{m}$; $S_{gb}=5000\text{cm}.\text{s}^{-1}$

Figure 4 showed that, for a given curve, the photocurrent decreases with an increase of the photovoltage. The increase of the grain radius leads to an increase of both of the magnitude of the photocurrent and the open circuit voltage.

This is due to the fact that increasing the grain radius minimizes recombination, which leads to a storage of charges in the base which increases photocurrent and photovoltage. The more the grain radius increases, the more the current and voltage output increases and the solar cell is of good quality.

Figure 5 showed that P-V characteristic curve is similar to those obtained using the columnar cubic grain [6]. It confirms the existence of the maximum power point (P_m) which is related to the “knee” of the I-V characteristic curve as it can be seen in [6], open-circuit point voltage and effect of grain size as shown by [6]. It is noted that P_m and V_{co} increase with the grain radius (R) corresponding to an increase of the fill factor (FF).

We have concluded with our model that the open circuit operating point is brief contrarily to the short-circuit operating condition. The shunt resistance is hence predominant and can be determined using our model. Based on previous findings, our cylindrical orientation model is not useful for the determination of the series resistance. For higher value of the dynamic junction velocity a ($S_f > 10^4\text{ cm/s}$), the shunt resistance R_{sh} depends on the photovoltage (V), the short-circuit photocurrent density (I_{sc}) and the photocurrent density (J_{ph}) [12].

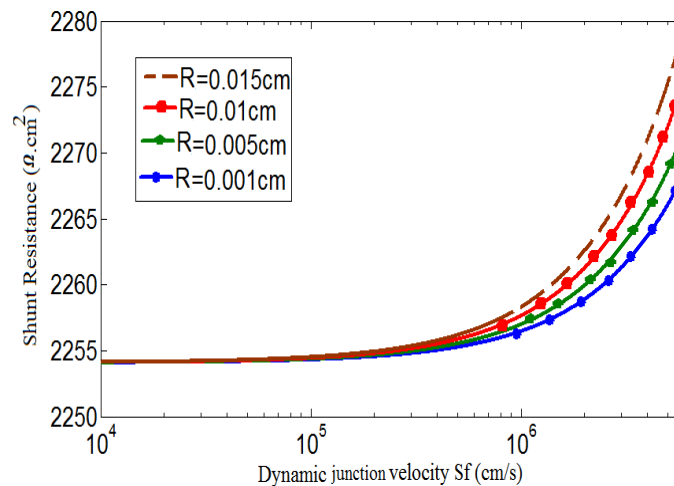


Figure 6: Shunt Resistance versus dynamic junction velocity for different grain radius: $D=26\text{cm}^2.\text{s}^{-1}$, $S_b=10^4\text{ cm}.\text{s}^{-1}$, $\lambda=1000\text{ nm}$, $L = 0.01\text{cm}$, $H=130\text{ }\mu\text{m}$, $S_{gb}=5000\text{cm}.\text{s}^{-1}$

Hence we use the electric equivalent circuit defined by [13, 14, 15] and the expression of the shunt resistance can be written as:



$$R_{sh}(H, S_{gb}, Sf, \lambda) = \frac{V_{ph}(H, S_{gb}, Sf, \lambda)}{I_{sc}(H, S_{gb}, Sf, \lambda) - I_{ph}(H, S_{gb}, Sf, \lambda)} \quad (11)$$

The profile of the shunt resistance versus dynamic junction velocity for different grain radius is given in figure 6.

Figure 6 showed an increase of the shunt resistance with the dynamic junction velocity, in the short-circuit zone, corresponding to a high short-circuit photocurrent. As shown in [6], the shunt resistance is related to manufacturing defects and poor solar cell design. Here, it is noted that the increase of the grain radius, corresponding to an increase of the grain size, lead to high shunt resistance. Our model confirms that the manufacturing defects and poor solar cell design could be avoided with high grain size.

4. Conclusion

A cylindrical model of a polycrystalline solar cell under monochromatic illumination is presented. The expression of the minority carriers' density allowed us to determine the photocurrent density and the photovoltage in function of the grain radius, the dynamic junction velocity, the wavelength and the grain boundary velocity. From the I-V and P-V characteristic curves, we deduce the shunt resistance of the solar cell. The effect of the grain radius has been noted on the above parameters. The high value of the grain radius is materialized by the increase of the volume of the solar cell and can be assimilated to that of monocrystalline silicon.

References

- [1]. W. Shockley, (1949). Dewice Electronics for Integrated Circuit, Bell Syst, Tech. J, 28, 435.
- [2]. G. Sissoko, C. Museruka, A. Correa, I. Gaye and A. L. Ndiaye (1996). Proc. of World Renewable Energy Congress, pp. 1487 – 1490, Denver, USA.
- [3]. H. L. Diallo, A. S. Maiga, A. Wereme and G. Sissoko (2008), J. Appl. Phys., Vol. 42, pp. 203- 211.
- [4]. S. Elnahwy and N. Adeeb (1988). Exact analysis of a three-dimensional cylindrical model for a polycrystalline solar cell. Journal of Applied Physics 64, 5214; doi: 10.1063/1.342435
- [5]. A. Trabelsi, A. Zouari and A. Ben Arab (2009). Modeling of polycrystalline N⁺/P junction solar cell with columnar cylindrical grain, Revue des Energies Renouvelables Vol. 12 N°2, 279 – 297
- [6]. G. Sissoko and S. Mbodji. (2011). A Method to Determine the Solar Cell Resistances from Single I-V Characteristic Curve Considering the Junction Recombination Velocity (Sf) International Journal of Pure and Applied Sciences and Technology, 6(2), pp. 103-114.
- [7]. S. Adachi, T. Kimura. And N. Suzuki. (1993). Optical Properties of CdTe: Experiment and Modelling, Journal of Applied Physics. 74, 3435-3441. <http://dx.doi.org/10.1063/1.354543>.
- [8]. S. Mbodji, M. Zoungrana, I. Zerbo, B. Dieng, G. Sissoko. Modelling Study of Magnetic Field's Effects on Solar Cell's Transient Decay, World Journal of Condensed Matter Physics, 2015, 5, 284-293.
- [9]. M. Thiame, H. Ly Diallo, M. M. Dione, Z. N. Bako, P. I. Ngom, M. Sane, A. G. Camara, A. Wereme, G. Sissoko. Etude en Modelisation à Trois Dimensions de l'Effet des Joints sur une Photopile à Jonction Verticale Série au Silicium Polycristallin. www.cadjds.org Journal des Sciences.
- [10]. I. Ly, M. Ndiaye, M. Wade, N. Thiam, S. Gueye, G. Sissoko. Concept of Recombination Velocity Sfcc At The Junction Of A Bifacial Silicon Solar Cell, In Steady State, Initiating The Short-Circuit Condition, Research Journal Of Applied Sciences, Engineering And Technology 5(1): 203-208, 2013.
- [11]. S. Mbodji, B. Mbow, F. I. Barro, and G. Sissoko, (2011), A 3D Model for Thickness and Diffusion Capacitance of Emitter-Base Junction Determination in a Bifacial Polycrystalline Solar Cell under Real Operating Condition. Turkish Journal of Physics, 35, 281-291.
- [12]. F. I Barro, S. Mbodji, M. Ndiaye, A. S. Maiga and G. Sissoko, Bulk and Surface recombination parameters measurement of silicon solar cell under constant white bias light, Journal des Sciences. J. Sci., 8(4): 37-41.
- [13]. Bashahu, M. and Habyarimana, (1995). Review and test of methods for determination of the solar cell series resistance. Renewable Energy, 6(2): 127-138.



- [14]. Bouzidi, K., M. Chegaar and A. Bouhemadou (2007). Solar cell parameters evaluation considering the series and shunt resistance, *Solar Energy Materials Solar Cells*, 91: 1647-1651.
- [15]. El-Adawi, M.K. and I.A Al-Nuaim (2002). A method to determine the solar cell series resistances from a single I-V characteristic curve considering its shunt resistance-new approach, *Vaccum*. 64: 33-36.

